Reprinted from the Proceedings of the 5th IFAC Symposium on Modelling and Control in Biomedical Systems, Melbourne, Australia, August 2003, pp. 359–363.

LATERAL-INHIBITORY-NETWORK MODELS OF TINNITUS

Ian C. Bruce[1], Harjeet S. Bajaj and Jennifer Ko

Department of Electrical and Computer Engineering,
McMaster University, 1280 Main Street West,
Hamilton, Ontario L8S 4K1, Canada

Abstract: Lateral-inhibitory-networks (LINs) of neurons enhance edges and peaks in their input excitation pattern. In the case of reduced spontaneous input to a region of a LIN, the edges between the normal and abnormal spontaneous input will be enhanced in the LIN's output. In LINs within the central auditory system, regional reduction of spontaneous input may occur because of deafferentation resulting from a peripheral hearing loss. A model of auditory LINs is developed to investigate how such abnormal spontaneous edges in LIN outputs could be related to tinnitus, the phantom perception of sounds. *Copyright © 2003 IFAC*

Keywords: Brain models, neural-network models, physiological models, dynamic systems, nonlinear systems, random processes.

1. INTRODUCTION

Lateral-inhibitory-networks (LINs) of neurons are thought to be widely used throughout the nervous system, including the auditory pathways of the brain (e.g., Shamma, 1985), to enhance spatial edges and peaks in their input excitation patterns. In the human auditory system, the inner ear maps the different frequency components of an acoustic signal onto a one-dimensional array of peripheral neurons. This is referred to as a tonotopic map. Processing of the peripheral excitation pattern by a LIN in the central nervous system will therefore enhance any edges and peaks in the frequency spectrum of an acoustic signal. However, if the spontaneous input to a region of the LIN (in the absence of sound-driven activity at that frequency) is reduced compared to the rest of the LIN, the edges between the normal and abnormal spontaneous input will be enhanced, giving rise to spuriously-enhanced edges in the LIN output.

Independent modelling studies by Gerken (1996) and Kral and Majernik (1996) investigated how such abnormal activity at the output of a LIN may be related to tinnitus, the phantom perception of sound. Both studies showed that a LIN receiving reduced spontaneous input over a restricted region may produce an output similar to that elicited by a tonal (or narrowband) acoustic input. It was consequently argued that this spontaneous tone-like output could be perceived as tinnitus.

However, both studies utilised highly-simplified models of the neurons in the LIN. In particular, neither model incorporated the temporal dynamics and spiking behaviour of a neural membrane. It is therefore difficult to assess whether their results apply to a LIN of real biological neurons.

In this paper, we develop a recurrent LIN of leaky integrate-and-fire neurons, which incorporate features of both the passive temporal dynamics and the active spiking and refractory behaviour of real biological neurons. It is found that the results of Gerken (1996) and Kral and Majernik (1996) are only obtained if the temporal dynamics (i.e., the membrane time-constant and the duration of excitatory and inhibitory synaptic currents) are slow enough and the rates of spontaneous inputs and outputs are fast enough that a high degree of temporal interaction is caused between the excitatory inputs and the recurrent lateral inhibitory inputs.

2. THE LATERAL-INHIBITORY-NETWORK MODEL

A schematic of the LIN is shown in Fig. 1. Each neuron in the LIN is described by an integrate-and-

[1] Email: ibruce@ieee.org

fire model. For a LIN consisting of n neurons, we define a column vector $\mathbf{v}$ of length n, where each element v_i is the membrane potential of neuron i in the LIN. For all subthreshold membrane potentials, i.e., for all $v_i(t)$ less than a constant threshold potential v_{thr} (= 1), the dynamics of the membrane potentials over time are described by the differential equation [e.g., Eq. (2) of Shamma, 1985]

$$\tau \frac{\mathrm{d}\,\mathbf{v}(t)}{\mathrm{d}\,t} + \mathbf{v}(t) = \mathbf{V}\mathbf{i}_{\mathrm{E}}(t) - \mathbf{W}\mathbf{i}_{\mathrm{I}}(t), \qquad (1)$$

where τ (= 5ms) is the membrane time constant, $\mathbf{v}(0) = 0$, $\mathbf{V}$ is an $n \times n$ matrix of excitatory synaptic weights, $\mathbf{W}$ is an $n \times n$ matrix of inhibitory synaptic weights, $\mathbf{i}_{\mathrm{E}}$ is a column vector of length n describing the excitatory synaptic input currents, and $\mathbf{i}_{\mathrm{I}}$ is a column vector of length n describing the inhibitory synaptic input currents.

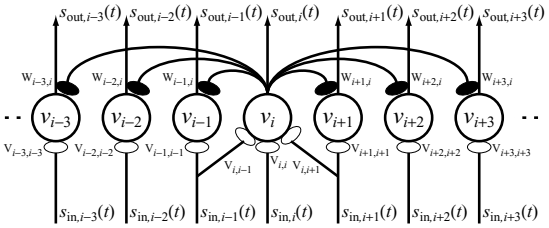

Fig. 1. Schematic of recurrent LIN. Excitatory synaptic inputs are shown by open ellipses and inhibitory synaptic inputs by filled ellipses. Input $s_{\mathrm{in}}(t)$ and output $s_{\mathrm{out}}(t)$ spike occurrences are convolved with unitary postsynaptic currents (not shown–see Fig. 2) and multiplied by the respective excitatory V_{ij} and inhibitory synaptic weights W_{ij} to produce excitatory $\mathbf{i}_{\mathrm{E}}$ and inhibitory $\mathbf{i}_{\mathrm{I}}$ input currents. Only convergent excitatory inputs onto neuron i and recurrent inhibitory inputs originating from neuron i are shown. Individual neurons are described by an integrate-and-fire model—see text for details.

Equation (1) was solved using a 4th-order Runge-Kutta algorithm with a fixed time-step Δt of 0.1 ms. Input spike instances $s_{\mathrm{in}}(t)$ were obtained using the Bernoulli approximation of a Poisson process (e.g., Edwards and Wakefield, 1990); $s_{\mathrm{in}}(t) = 1$ for discrete times $t = c\Delta t$ (where c = 0, 1, 2,…) during which a spike occurs and is zero otherwise. The j^{th} excitatory synaptic current at discrete times is obtained by convolving input spike instances $s_{\mathrm{in}}(t)$ for the j^{th} input with a unitary excitatory postsynaptic current (EPSC) waveform

$$i_{\mathrm{EPSC}}(t) = \left(\frac{\alpha_{\mathrm{EPSC}}}{10\tau}\right)^2 t \exp\left(-\alpha_{\mathrm{EPSC}}\, t/\tau\right), \quad (2)$$

as plotted in Fig. 2. This type of equation is known as an alpha function; the greater the value of α_{EPSC} (= 5), the EPSC alpha value, the sharper the alpha function. In this formulation of the alpha function the electrical charge delivered, i.e., the area under the function, is independent of the alpha value.

The j^{th} inhibitory synaptic current is obtained by convolving $s_{\mathrm{out}}(t)$ from neuron j (see below) with the unitary inhibitory postsynaptic current (IPSC) waveform $i_{\mathrm{IPSC}}(t)$, which takes the same form as Eq. (2) but with the alpha value α_{IPSC} (= 1).

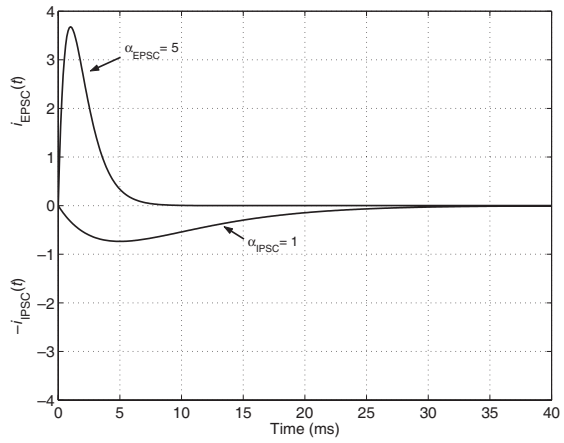

Fig. 2. Unitary postsynaptic currents. Excitatory input spike instances $s_{\mathrm{in}}(t)$ are convolved in time with $i_{\mathrm{IPSC}}(t)$ to create the excitatory input current $\mathbf{i}_{\mathrm{E}}$. Likewise, recurrent inhibitory output spike instances $s_{\mathrm{out}}(t)$ are convolved with $i_{\mathrm{IPSC}}(t)$ to create the inhibitory input current $\mathbf{i}_{\mathrm{I}}$.

For any discrete time t, if $v_i(t) \geq v_{\mathrm{thr}}$ then $v_i(t)$ is set to some arbitrarily-high value v_{sp} (= 5) to indicate a spike. v_i is then held at zero over the interval $[t + \Delta t, t + t_{\mathrm{ref}}]$, where t_{ref} (= 1 ms) is the absolute refractory period. Output spike instances $s_{\mathrm{out}}(t)$ are also recorded for each neuron i. The j^{th} inhibitory synaptic current is then obtained by convolving $s_{\mathrm{out}}(t)$ from neuron j with $i_{\mathrm{EPSC}}(t)$. Consequently, $\mathbf{i}_{\mathrm{I}}$ is a nonlinear function of the vector of neural membrane potentials $\mathbf{v}$. Such a system with inhibitory feedback is referred to as a *recurrent* LIN.

Each element of the synaptic weight matrices, V_{ij} for excitatory inputs and W_{ij} for inhibitory inputs, corresponds to the effectiveness of the j^{th} synaptic current on neuron i. In this paper, $\mathbf{V}$ is set to the identity matrix $\mathbf{I}$, such that neuron i only receives excitation from the j^{th} input spike train for $j = i$. For the inhibitory synaptic weight matrix, each element W_{ij} is set to zero for $j = i$, i.e., neurons do not inhibit themselves, and each neuron i receives inhibitory inputs from k neighbouring neurons on each side. In this paper, the weights W_{ij} for $j = i - k \ldots i - 1$ and $j = i + 1 \ldots i + k$ are set to a Gaussian window function of length k = 5, as shown in Fig. 3 (*cf.* Fig.3 of Gerken, 1996). The absolute values of W_{ij} are scaled so that the sum of the inhibitory weights for each neuron $\sum_{j=1}^{n} W_{ij}$ is equal to two. Consequently, if a

neuron were to receive identical excitatory and inhibitory currents on all its inputs simultaneously, it would receive two times as much inhibitory drive as excitatory drive. However, the inhibitory drive is distributed across $2k$ synapses receiving spikes from recurrent lateral connections independently over time, and consequently the inhibitory drive is typically somewhat less than the excitatory drive. Having slightly more excitatory than inhibitory drive allows enhancement of edges and peaks without producing distortions of flat regions of the excitation pattern (see. Figs. 4–7). For neurons at and near the edges of the LIN, i.e, $i \le k$ or $i \ge n - k$, the number of recurrent inhibitory inputs must be reduced because neighbouring neurons will be lacking on one side. In these cases, the weights of the existing inhibitory synapses are increased so as to match the total inhibitory input for neurons in middle sections of the LIN, removing confounding edge effects.

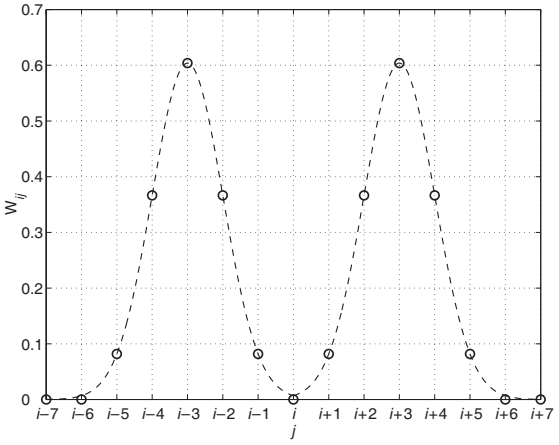

Fig. 3. Inhibitory weights W_{ij} (open circles) for neuron i and the j^{th} recurrent output spike train. W_{ij} is zero for $j = i$, obeys a Gaussian window function (dashed line) for recurrent inputs from the k (= 5) neighbouring neurons on each side, and is zero elsewhere.

3. RESULTS

Simulations of LINs containing 200 integrate-and-fire neurons receiving Poisson-distributed spike inputs were performed in MATLAB (MathWorks, Natick, MA). These neurons were assumed to have best frequencies (BFs) over the range 0 to 10 kHz corresponding to linear spacing on the basilar membrane (Greenwood, 1990).

Figure 4 shows mean spike rates for the LIN inputs and outputs for a case of spike inputs arising from normal hearing. The spontaneous input rate is 50 spikes/s for all neurons, and input spike rates are elevated (max = 250 spikes/s) around BF = 5.5 kHz, simulating a pure-tone acoustic stimulus at that frequency. The spontaneous output spike rate is around 25 spikes/s, reduced from 50 spikes/s because of both the recurrent inhibitory inputs and the refractory behaviour of the integrate-and-fire neuron. The lateral inhibitory behaviour produces contrast enhancement of the excitatory peak at 5.5 kHz–note the dips approaching zero in the mean output spike rate around 5 and 6 kHz.

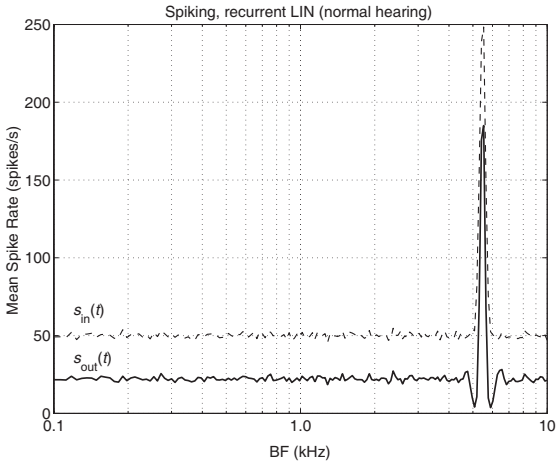

Fig. 4. Mean spike rates for LIN inputs $s_{\text{in}}(t)$ (thin dashed line) and outputs $s_{\text{out}}(t)$ (thick solid line) for a case of normal hearing, with spontaneous input rates of 50 spikes/s and a pure-tone acoustic stimulus at 5.5 kHz.

A case of abnormal spontaneous input to the LIN is simulated in Fig. 5 for a high-frequency hearing loss above 1.1 kHz. The spontaneous input rate is 50 spikes/s for neurons in the normal region below 1.1 kHz, but the spontaneous rate is reduced to 20 spikes/s for neurons in the region of hearing loss, producing an edge in the spontaneous excitation pattern. A pure-tone acoustic stimulus of 5.5 kHz still produces elevated (max = 250 spikes/s) input spike rates around that BF. As well as the contrast enhancement of the excitatory peak at 5.5 kHz, the LIN now produces a small peak at the low frequency side of the edge between the regions of normal and impaired hearing (indicated by the arrow), with a small corresponding dip on the high frequency side of the edge.

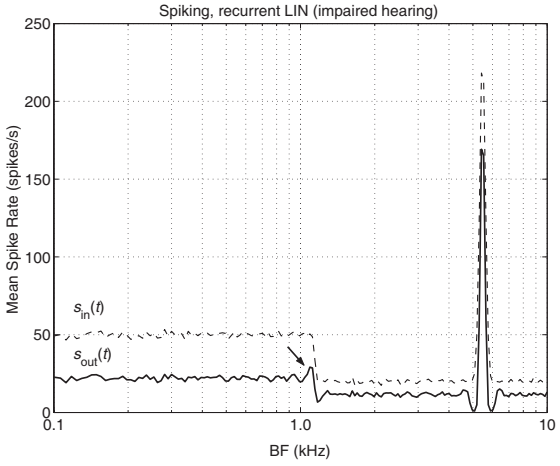

Fig. 5. Mean spike rates for LIN inputs $s_{\text{in}}(t)$ (thin dashed line) and outputs $s_{\text{out}}(t)$ (thick solid line) for a case of impaired hearing, with spontaneous input rates of 50 spikes/s in the region of normal hearing and 20 spikes/s in the region of high-frequency hearing loss, and a pure-tone acoustic stimulus at 5.5 kHz.

The peak in Fig. 5 is quite small and consequently may be barely distinguishable from the background spontaneous activity. In Figs. 6 and 7 we consider cases where the normal spontaneous input rates are increased to 100 spikes/s and 200 spikes/s, respectively. In each case, the size of the spurious peak of excitation (indicated by the arrows) is progressively increased, such that it is clearly discernible from the flanking spontaneous activity in the normal hearing region and begins to look more like a peak of activity due to a pure-tone acoustic stimulus.

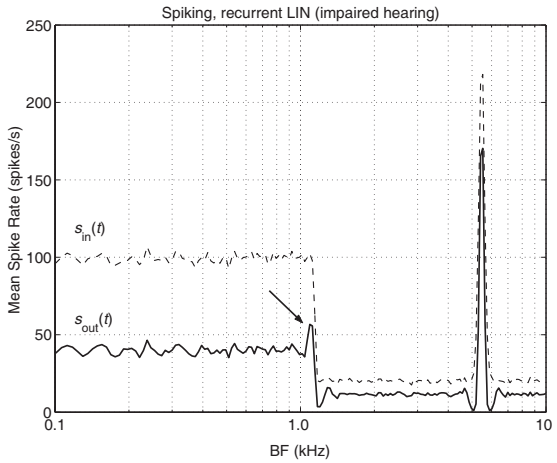

Fig. 6. Elevated spontaneous input in the region of normal hearing: mean spike rates for LIN inputs $s_{in}(t)$ (thin dashed line) and outputs $s_{out}(t)$ (thick solid line) for a case of impaired hearing, with spontaneous input rates of **100 spikes/s** in the region of normal hearing (*cf.* 50 spikes/s in Fig. 5) and 20 spikes/s in the region of high-frequency hearing loss, and a pure-tone acoustic stimulus at 5.5 kHz.

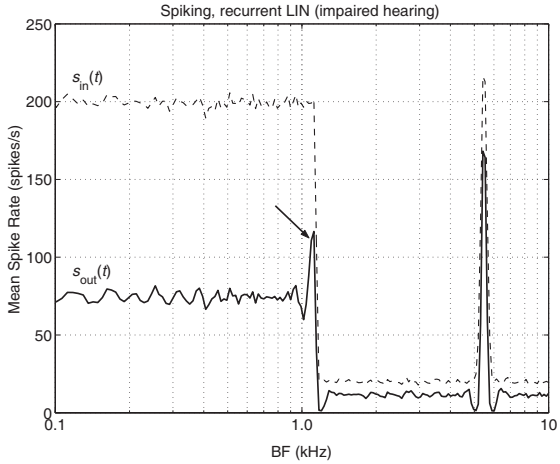

Fig. 7. Highly elevated spontaneous input in the region of normal hearing: mean spike rates for LIN inputs $s_{in}(t)$ (thin dashed line) and outputs $s_{out}(t)$ (thick solid line) for a case of impaired hearing, with spontaneous input rates of 2**00 spikes/s** in the region of normal hearing (*cf.* 50 spikes/s in Fig. 5 and 100 spikes/s in Fig. 6) and 20 spikes/s in the region of high-frequency hearing loss, and a pure-tone acoustic stimulus at 5.5 kHz.

4. DISCUSSION AND CONCLUSIONS

In this paper, a recurrent, spiking LIN was developed to illustrate the effects of reduced spontaneous input activity for a region of the LIN. The results are generally consistent with those of Gerken (1996) and Kral and Majernik (1996), who found that simpler nonrecurrent, non-spiking LIN models produce a substantial enhancement of the edge between the normal and reduced spontaneous input activity. However, with the recurrent, spiking LIN developed in this paper, we found that the degree of edge enhancement was quite dependent on the mean input and output spike rates in the normal region of spontaneous activity. This dependence indicates that the effectiveness of the LIN in enhancing edges (and peaks) is governed by the amount of inhibitory interaction between neighbouring neurons. Even though all these simulations were carried out with fairly slow temporal dynamics (τ = 5ms and the excitatory and inhibitory postsynaptic currents last around 5 ms and 20 ms, respectively), substantial enhancement of the edge of the hearing loss is only obtained when the input and output spike rates in the region of normal hearing are high enough to create significant temporal overlap between the excitatory and inhibitory currents.

If the temporal dynamics are sped up or if the output spike rates are reduced by lowering the input rates, increasing the membrane threshold potential, or extending the duration of the refractory period, there will be fewer interactions between the excitatory and inhibitory inputs. For example, output discharge rates are lower than input discharge rates, and consequently the rate of recurrent inhibitory synaptic events is lower than the rate of excitatory synaptic events. Therefore we set the inhibitory postsynaptic current duration to be substantially longer than the excitatory current duration in these simulations (around 20 ms and 5 ms, respectively) to increase the opportunities for inhibitory interactions between neurons. However, physiological evidence for longer lateral-inhibitory synaptic currents in the auditory midbrain or cortex is not strong (e.g., Depireux et al., 2001; Escabi and Schreiner, 2002)

In the case of a normal spontaneous input rate of 200 spikes/s (Fig. 7), a large peak at the edge of the hearing loss was produced at the output of the LIN. Following Gerken (1996) and Kral and Majernik (1996), we postulate that the spurious peak in the output excitation pattern of the LIN may be a neural generator of tinnitus, the phantom perception of a sound. While a spontaneous input rate of 200 synaptic events per second from a single synapse is unlikely, it may be possible for multiple independent synaptic inputs to add together to create a total spontaneous input rate of 200 events/s or greater. However, the feasibility of this remains to be determined from anatomical and physiological studies of LINs in the central auditory system. Such investigations are also necessary to ascertain the accuracy of the time scales of the neural dynamics used in this paper, i.e., the membrane time constant

and the time courses of excitatory and inhibitory postsynaptic currents.

In this paper we have only investigated the acute effects of abnormal spontaneous input to a LIN—no plastic changes in synaptic weights due to input or output activity was considered. However, there exists both physiological and psychophysical evidence that many forms of tinnitus develop over the course of hours to days (e.g., Kaltenbach, 200), suggesting that neural plasticity may play an important role. Therefore, the effects of plastic changes in synaptic weights will be examined in future modelling studies. For these investigations, it will be important to study the consequences of sound-driven auditory-nerve activity from the normal and impaired ear (Bruce et al., 2003), in addition to spontaneous input activity. The patterns of driven input activity will be greatly different to those of the spontaneous activity and may have a profound impact on any plastic changes in the LIN synaptic weights.

ACKNOWLEDGEMENTS

This research was supported by the Canadian Institutes of Health Research (NET 54023).

REFERENCES

Bruce, I.C., M.B. Sachs and E.D. Young (2003). An auditory-periphery model of the effects of acoustic trauma on auditory nerve responses. *J. Acoust. Soc. Am.*, **113**, 369–388.

Depireux D.A., J.Z. Simon, D.J. Klein and S.A. Shamma (2001). Spectro-temporal response field characterization with dynamic ripples in ferret primary auditory cortex. *J. Neurophysiol.*, **85**, 1220–1234.

Edwards, B.W. and G.H. Wakefield (1990). On the statistics of binned neural point processes: the Bernoulli approximation and AR representation of the PST histogram. *Biol. Cybern.,* **64,** 145–153.

Escabi, M.A. and C.E. Schreiner (2002). Nonlinear spectrotemporal sound analysis by neurons in the auditory midbrain. *J. Neurosci.*, **22**, 4114–4131.

Gerken, G.M. (1996). Central tinnitus and lateral inhibition: an auditory brainstem model. *Hear. Res.,* **97,** 75–83.

Greenwood, D.D. (1990). A cochlear frequency-position function for several species–29 years later. *J. Acoust. Soc. Am.,* **87,** 2592–2605.

Kaltenbach, J.A. (2000). Neurophysiologic mechanisms of tinnitus. *J. Am. Acad. Audiol.*, **11**, 125–137.

Kral, A. and V. Majernik (1996). On lateral inhibition in the auditory system. *Gen. Physiol. Biophys.,* **15,** 109–127.

Shamma, S.A. (1985). Speech processing in the auditory system II: Lateral inhibition and the central processing of speech evoked activity in the auditory nerve. *J. Acoust. Soc. Am.,* **78,** 1622–1632.